Communications in Applied and Industrial Mathematics, DOI: 10.1685/journal.caim.374
ISSN 2038-0909, e-374

Fast and effective finite difference method for 2D photonic crystals

Pietro Contu, Cornelis van der Mee, Sebastiano Seatzu

Dip. Matematica e Informatica, Università di Cagliari
Viale Merello 92, 09123 Cagliari, Italy
contu22@interfree.it
cornelis@krein.unica.it
seatzu@unica.it

Communicated by Nicola Bellomo

Abstract

In this article we develop a finite difference (FDFD) method to compute the band spectra of 2D photonic crystals without impurities. Exploiting periodicity to identify discretization points differing by a period, the computational complexity of the algorithms is reduced significantly. Numerical results on three test problems are presented.

Keywords: `2D photonic crystals, finite difference method, band spectra, 2D Helmholtz equation.`

AMS Subject Classification: `78M20`

1. Introduction.

Two-dimensional (2D) pure photonic crystals [1,2] are dielectric media whose dielectric constant ε only depends on $\boldsymbol{x} = (x, y) \in \mathbb{R}^2$ and not on the third cartesian coordinate z and, for certain linearly independent vectors $\boldsymbol{a}_1, \boldsymbol{a}_2 \in \mathbb{R}^2$, satisfies the periodicity condition

$$\varepsilon(\boldsymbol{x} + m_1\boldsymbol{a}_1 + m_2\boldsymbol{a}_2) = \varepsilon(\boldsymbol{x}), \qquad \boldsymbol{x} = (x, y) \in \mathbb{R}^2, \tag{1}$$

where m_1 and m_2 are arbitrary integers. Letting c be the speed of light, ω the angular frequency of the harmonic mode, and $\eta = (\omega/c)^2$, in the transverse magnetic (TM) mode the electric field ψ satisfies the Helmholtz equation [3]

$$-\nabla^2\psi = \eta\varepsilon\psi, \tag{2}$$

whereas in the transverse electric (TE) mode the magnetic field ψ satisfies

$$-\nabla \cdot \left(\frac{1}{\varepsilon}\nabla\psi\right) = \eta\psi. \tag{3}$$

Received 2011 08 04. Accepted 2011 08 26. Published 2011 11 28.

In either mode the field ψ points in the z-direction and only depends on $(x, y) \in \mathbb{R}^2$. Using the Bloch representation

$$\psi(\boldsymbol{x}, \boldsymbol{k}) = e^{i\boldsymbol{k}\cdot\boldsymbol{x}}\phi(\boldsymbol{x}, \boldsymbol{k}),$$

where the wavevector $\boldsymbol{k}$ belongs to the first Brillouin zone [4] and ϕ satisfies the periodicity condition

$$\phi(\boldsymbol{x} + m_1\boldsymbol{a}_1 + m_2\boldsymbol{a}_2, \boldsymbol{k}) = \phi(\boldsymbol{x}, \boldsymbol{k}) \tag{4}$$

for any $m_1, m_2 \in \mathbb{Z}$, we obtain instead of (2) and (3) the equations

$$-\nabla^2\phi - 2i\boldsymbol{k}\cdot\nabla\phi + \|\boldsymbol{k}\|^2\phi = \eta\varepsilon\phi \tag{5}$$

for TM modes and

$$-\nabla\cdot\left(\frac{1}{\varepsilon}\nabla\phi\right) - i\nabla\cdot\left(\frac{1}{\varepsilon}\boldsymbol{k}\phi\right) - i\frac{1}{\varepsilon}\boldsymbol{k}\cdot\nabla\phi + \frac{\|\boldsymbol{k}\|^2}{\varepsilon}\phi = \eta\phi \tag{6}$$

for TE modes. Throughout the paper, $\|\cdot\|$ denotes the euclidean norm.

In the literature the photonic band spectra have been computed by two basic families of methods: time domain methods and frequency domain methods. The first is based on the numerical solution of a wave equation followed by a Fourier analysis in the time variable to extract the spectrum. In the frequency domain methods the band spectra are obtained by the numerical solution of a Helmholtz-like equation for a selection of wavevectors $\boldsymbol{k}$. These numerical methods have been applied to a variety of model 2D photonic crystals, where each elementary cell consists of two distinct dielectrically homogeneous materials, one forming an array of circles, squares, or honey comb and the other being the background. We mention time domain applications using the plane wave expansion (PWE) [5–10] and finite difference time domain (FDTD) [11–17] methods and frequency domain applications using the finite difference frequency domain (FDFD) [18–20], finite element frequency domain (FEFD) [21–29], multiple scattering (MS) [30–33], and Fourier expansion (FE) [1,34,35] methods.

In this article we develop a finite difference domain (FDFD) method to compute the spectra of the Helmholtz-like equations (5) and (6) for fixed $\boldsymbol{k} \in \mathbb{R}^2$. When varying $\boldsymbol{k}$ over the first Brillouin zone or any part of it depending on the rotation and reflection symmetries of $\varepsilon(\boldsymbol{x})$, we obtain the band spectra for the TM and TE modes for given dielectric constant. Choosing positive integers n, m and the division points

$$\boldsymbol{x}_{j,l} = (j/n)\boldsymbol{a}_1 + (l/m)\boldsymbol{a}_2, \qquad (j, l) \in \mathbb{Z}^2, \tag{7}$$

DOI: 10.1685/journal.caim.374

we can convert the finite difference frequency domain (FDFD) scheme for (5) and (6) into linear systems of the type

$$(C - \eta D)\boldsymbol{\phi}, \tag{8}$$

where C and D are sparse positive definite matrices of order nm. The periodicity condition (4) has been employed to identify the values of ϕ at the division points $\boldsymbol{x}_{j,l}$ and $\boldsymbol{x}_{j',l'}$ whenever $j - j'$ is an integer multiple of n and $l - l'$ an integer multiple of m. Partial results have been obtained before in [36].

The numerical results have been obtained, in either mode, by the FDFD method and compared with results obtained using the Fourier expansion method of Joannopoulos et al. [1]. In Sec. 2 we shall discuss our implementation of the FDFD method in detail, first for rectangular 2D crystals (where $\boldsymbol{a}_1 \cdot \boldsymbol{a}_2 = 0$) and then for oblique 2D crystals, in either mode. In Sec. 3 we discuss the circulant-diagonal matrix systems. In Sec. 4 we present our numerical results and in Sec. 5 our conclusions.

2. Finite difference frequency domain.

In this section we discuss the finite difference method [37–39] in the frequency domain to determine the spectra of 2D photonic crystals.

a. Rectangular photonic crystals. Let us formulate our FDFD method first for rectangular 2D crystals, where $\boldsymbol{a}_1 = (a, 0)$ and $\boldsymbol{a}_2 = (0, b)$. Defining the division points as in (7), putting $h_x = (a/n)$, $h_y = (b/m)$, $\phi_{j,l} = \phi(\boldsymbol{x}_{j,l})$, and $\varepsilon_{j,l} = \varepsilon(\boldsymbol{x}_{j,l})$ for any $(j, l) \in \mathbb{Z}^2$, collocating (5) (TM mode) in $\boldsymbol{x}_{j,l}$, and discretizing by the usual central scheme, we obtain the finite difference equation

$$\begin{aligned} &- \frac{\phi_{j+1,l} - 2\phi_{j,l} + \phi_{j-1,l}}{h_x^2} - \frac{\phi_{j,l+1} - 2\phi_{j,l} + \phi_{j,l-1}}{h_y^2} \\ &- 2ik_x \frac{\phi_{j+1,l} - \phi_{j-1,l}}{2h_x} - 2ik_y \frac{\phi_{j,l+1} - \phi_{j,l-1}}{2h_y} + [k_x^2 + k_y^2]\phi_{j,l} \\ &= \eta \varepsilon_{j,l} \phi_{j,l}, \end{aligned} \tag{9}$$

where $\boldsymbol{k} = (k_x, k_y)$ is a fixed wavevector in the first Brillouin zone. The periodicity conditions (1) and (4) on the dielectric constant and the Bloch corrected field allow us to make the identifications

$$\varepsilon_{j,l} = \varepsilon_{j',l'}, \qquad \phi_{j,l} = \phi_{j',l'},$$

whenever $(j - j')/n$ and $(l - l')/m$ are integers. As a result, we can convert (9) into a linear system of the form (8) of order nm satisfied by the column

vector with components $\phi_{j,l}$ for the following (j,l):

$$(10)\qquad \begin{cases} (j,l), & j=1,\ldots,n-1,\ l=1,\ldots,m-1,\\ (0,l), & l=1,\ldots,m-1,\\ (j,0), & j=1,\ldots,n-1,\\ (0,0). \end{cases}$$

Notice that this procedure is equivalent to discretizing (5) on the two-dimensional torus.

The finite difference scheme for (6) (TE mode) is less straightforward, because the presence of the function $(1/\varepsilon)$ in the differential operator in situations where the physics of the problem requires $(1/\varepsilon)$ to have jump discontinuities, requires some averaging of $(1/\varepsilon)$. The finite difference scheme used in the TE mode is the following:

$$\begin{aligned} &-\tfrac{1}{2}\left(\frac{1}{\varepsilon_{j+1,l}}+\frac{1}{\varepsilon_{j,l}}\right)\frac{\phi_{j+1,l}-\phi_{j,l}}{h_x^2}-\tfrac{1}{2}\left(\frac{1}{\varepsilon_{j,l}}+\frac{1}{\varepsilon_{j-1,l}}\right)\frac{\phi_{j,l}-\phi_{j-1,l}}{h_x^2}\\ &-\tfrac{1}{2}\left(\frac{1}{\varepsilon_{j,l+1}}+\frac{1}{\varepsilon_{j,l}}\right)\frac{\phi_{j,l+1}-\phi_{j,l}}{h_y^2}-\tfrac{1}{2}\left(\frac{1}{\varepsilon_{j,l}}+\frac{1}{\varepsilon_{j,l-1}}\right)\frac{\phi_{j,l}-\phi_{j,l-1}}{h_y^2}\\ &-ik_x\frac{\frac{1}{\varepsilon_{j+1,l}}\phi_{j+1,l}-\frac{1}{\varepsilon_{j-1,l}}\phi_{j-1,l}}{2h_x}-ik_y\frac{\frac{1}{\varepsilon_{j,l+1}}\phi_{j,l+1}-\frac{1}{\varepsilon_{j,l-1}}\phi_{j,l-1}}{2h_y}\\ &-ik_x\frac{\frac{1}{\varepsilon_{j,l}}\phi_{j+1,l}-\frac{1}{\varepsilon_{j,l}}\phi_{j-1,l}}{2h_x}-ik_y\frac{\frac{1}{\varepsilon_{j,l}}\phi_{j,l+1}-\frac{1}{\varepsilon_{j,l-1}}\phi_{j,l}}{2h_y}\\ &+\tfrac{1}{4}k_x^2\left(\frac{1}{\varepsilon_{j+1,l}}+\frac{2}{\varepsilon_{j,l}}+\frac{1}{\varepsilon_{j-1,l}}\right)\phi_{j,l}+\tfrac{1}{4}k_y^2\left(\frac{1}{\varepsilon_{j,l+1}}+\frac{2}{\varepsilon_{j,l}}+\frac{1}{\varepsilon_{j,l-1}}\right)\phi_{j,l}\\ &=\eta\phi_{j,l}, \end{aligned}\qquad (11)$$

where $\boldsymbol{k}=(k_x,k_y)$. Equation (11) is easily written in the form

$$\begin{aligned} &\tfrac{1}{2}\left(\frac{1}{\varepsilon_{j+1,l}}+\frac{1}{\varepsilon_{j,l}}\right)\left[-\frac{1}{h_x^2}-\frac{ik_x}{h_x}\right]\phi_{j+1,l}+\tfrac{1}{2}\left(\frac{1}{\varepsilon_{j,l}}+\frac{1}{\varepsilon_{j-1,l}}\right)\left[-\frac{1}{h_x^2}+\frac{ik_x}{h_x}\right]\phi_{j-1,l}\\ &+\tfrac{1}{2}\left(\frac{1}{\varepsilon_{j,l+1}}+\frac{1}{\varepsilon_{j,l}}\right)\left[-\frac{1}{k_y^2}-\frac{ik_y}{h_y}\right]\phi_{j,l+1}+\tfrac{1}{2}\left(\frac{1}{\varepsilon_{j,l}}+\frac{1}{\varepsilon_{j,l-1}}\right)\left[-\frac{1}{h_y^2}+\frac{ik_y}{h_y}\right]\phi_{j,l-1}\\ &+\left\{\tfrac{1}{4}\left(\frac{1}{\varepsilon_{j+1,l}}+\frac{2}{\varepsilon_{j,l}}+\frac{1}{\varepsilon_{j-1,l}}\right)\left[\frac{2}{h_x^2}+k_x^2\right]\right.\\ &\left.+\tfrac{1}{4}\left(\frac{1}{\varepsilon_{j,l+1}}+\frac{2}{\varepsilon_{j,l}}+\frac{1}{\varepsilon_{j,l-1}}\right)\left[\frac{2}{h_y^2}+k_y^2\right]\right\}\phi_{j,l}=\eta\phi_{j,l}. \end{aligned}\qquad (12)$$

DOI: 10.1685/journal.caim.374

Equations (9) and (12) can both be written in the form (8), where C is a positive semidefinite hermitian matrix and D is a diagonal matrix with positive diagonal entries. In the case of (12), D is the identity matrix of order mn. In the case of (9), C is a two-index circulant matrix, i.e., its entries $C_{(j,l),(j',l')}$ only depend on the remainders of $j-j'$ and $l-l'$ upon division by n and m, respectively. In that case the eigenvalues of C are given by the symbol [40–42]

$$\begin{aligned} &k_x^2+k_y^2+\frac{2}{h_x^2}(1-\cos\theta_j)+\frac{2k_x}{h_x}\sin\theta_j+\frac{2}{h_y^2}(1-\cos\varphi_l)+\frac{2k_y}{h_y}\sin\varphi_l \\ &=\left(k_x+\frac{\sin\theta_j}{h_x}\right)^2+\left(k_y+\frac{\sin\varphi_l}{h_y}\right)^2+\frac{(1-\cos\theta_j)^2}{h_x^2}+\frac{(1-\cos\varphi_l)^2}{h_y^2} \\ &=\left(k_x+\frac{2\pi j}{a}\right)^2+\left(k_y+\frac{2\pi l}{b}\right)^2+O(n^{-2}+m^{-2}), \end{aligned} \tag{13}$$

where $\theta_j=(2\pi j/n)$ $(j=0,1,\dots,n-1)$ and $\varphi_l=(2\pi l/m)$ $(l=0,1,\dots,m-1)$. The expression (13) is easily seen to be nonnegative and to vanish if and only if $k_x=k_y=j=l=0$. In the case of (12), after some algebra and using that $\varepsilon_{j,l}$ and $\phi_{j,l}$ only depend on the remainders of j and l upon division by n and m, we get

$$\begin{aligned} \eta\sum_{j,l}|\phi_{j,l}|^2=\sum_{j,l}\tfrac{1}{4}\left(\frac{1}{\varepsilon_{j+1,l}}+\frac{1}{\varepsilon_{j,l}}\right)\Bigg\{&\left(\sqrt{\frac{1}{h_x^2}+k_x^2}-\frac{1}{h_x}\right)^2[|\phi_{j,l}|^2+|\phi_{j+1,l}|^2] \\ &+\frac{2}{h_x}|\phi_{j,l}-e^{i\omega_x}\phi_{j+1,l}|^2\sqrt{\frac{1}{h_x^2}+k_x^2}\Bigg\} \\ +\sum_{j,l}\tfrac{1}{4}\left(\frac{1}{\varepsilon_{j,l+1}}+\frac{1}{\varepsilon_{j,l}}\right)\Bigg\{&\left(\sqrt{\frac{1}{h_y^2}+k_y^2}-\frac{1}{h_y}\right)^2[|\phi_{j,l}|^2+|\phi_{j,l+1}|^2] \\ &+\frac{2}{h_y}|\phi_{j,l}-e^{i\omega_y}\phi_{j,l+1}|^2\sqrt{\frac{1}{h_y^2}+k_y^2}\Bigg\}, \end{aligned}$$

where for suitable phases $\omega_x,\omega_y\in\mathbb{R}$

$$\frac{1}{h_x^2}+\frac{ik_x}{h_x}=\frac{1}{h_x}e^{i\omega_x}\sqrt{\frac{1}{h_x^2}+k_x^2},\quad \frac{1}{h_y^2}+\frac{ik_y}{h_y}=\frac{1}{h_y}e^{i\omega_y}\sqrt{\frac{1}{h_y^2}+k_y^2}.$$

As a result, in the case of (12), the matrix C is positive definite hermitian and zero is an eigenvalue if and only if $k_x=k_y=0$.

b. Oblique photonic crystals. If the 2D photonic crystal is oblique, we enact the coordinate transformation

$$\boldsymbol{x} = \mathrm{col}(\boldsymbol{a}^1, \boldsymbol{a}^2)\boldsymbol{\xi} = \begin{pmatrix} a_{11} & a_{21} \\ a_{12} & a_{22} \end{pmatrix} \begin{pmatrix} \xi \\ \zeta \end{pmatrix} = A^T \boldsymbol{\xi}, \tag{14}$$

where ξ and ζ are orthogonal coordinates and $\boldsymbol{a}^1$ and $\boldsymbol{a}^2$ denote the transposed rows of A. Then

$$\begin{pmatrix} \xi \\ \zeta \end{pmatrix} = \frac{1}{2\pi}\mathrm{col}(\boldsymbol{b}_1, \boldsymbol{b}_2)\boldsymbol{x} = \frac{1}{2\pi} \begin{pmatrix} b_{11} & b_{12} \\ b_{21} & b_{22} \end{pmatrix} \boldsymbol{x} = \frac{1}{2\pi} B\boldsymbol{x},$$

where $\boldsymbol{b}_1$ and $\boldsymbol{b}_2$ are the so-called reciprocal basis vectors, which implies $A^T B = 2\pi I_2$. Using that

$$\begin{aligned} \boldsymbol{k} \cdot \nabla\phi &= \frac{1}{2\pi}(B\boldsymbol{k}) \cdot \nabla_{\boldsymbol{\xi}}\phi, \\ \nabla^2\phi &= \frac{1}{4\pi^2}\left(\|\boldsymbol{b}^1\|^2 \frac{\partial^2\phi}{\partial\xi^2} + \|\boldsymbol{b}^2\|^2 \frac{\partial^2\phi}{\partial\zeta^2} + 2\boldsymbol{b}^1 \cdot \boldsymbol{b}^2 \frac{\partial^2\phi}{\partial\xi\partial\zeta} \right), \end{aligned}$$

and putting $\tilde{\phi}(\boldsymbol{\xi}) = \phi(A^{-1}\boldsymbol{x})$, we get instead of (5) (TM mode)

$$\begin{aligned} &- \frac{1}{4\pi^2}\left(\|\boldsymbol{b}^1\|^2 \frac{\partial^2\tilde{\phi}}{\partial\xi^2} + \|\boldsymbol{b}^2\|^2 \frac{\partial^2\tilde{\phi}}{\partial\zeta^2} + 2\boldsymbol{b}^1 \cdot \boldsymbol{b}^2 \frac{\partial^2\tilde{\phi}}{\partial\xi\partial\zeta} \right) \\ &- \frac{i}{\pi}(B\boldsymbol{k}) \cdot \nabla_{\boldsymbol{\xi}}\tilde{\phi} + \|\boldsymbol{k}\|^2\tilde{\phi}(\boldsymbol{\xi}) = \eta\,\tilde{\varepsilon}(\boldsymbol{\xi})\tilde{\phi}(\boldsymbol{\xi}), \end{aligned} \tag{15}$$

where $\tilde{\varepsilon}(\boldsymbol{\xi}) = \varepsilon(A^T\boldsymbol{\xi})$ and $\boldsymbol{b}^1$ and $\boldsymbol{b}^2$ are the transposed row vectors of B.

Instead of (6) (TE mode) we obtain

$$\begin{aligned} &- \frac{1}{4\pi^2}\boldsymbol{b}_1 \cdot \nabla_{\boldsymbol{\xi}}\left(\frac{\boldsymbol{b}_1 \cdot \nabla_{\boldsymbol{\xi}}\tilde{\phi}}{\tilde{\varepsilon}} \right) - \frac{1}{4\pi^2}\boldsymbol{b}_2 \cdot \nabla_{\boldsymbol{\xi}}\left(\frac{\boldsymbol{b}_2 \cdot \nabla_{\boldsymbol{\xi}}\tilde{\phi}}{\tilde{\varepsilon}} \right) \\ &- \frac{ik_1}{2\pi}\boldsymbol{b}_1 \cdot \nabla_{\boldsymbol{\xi}}\left(\frac{\tilde{\phi}}{\tilde{\varepsilon}} \right) - \frac{ik_2}{2\pi}\boldsymbol{b}_2 \cdot \nabla_{\boldsymbol{\xi}}\left(\frac{\tilde{\phi}}{\tilde{\varepsilon}} \right) + \frac{\|\boldsymbol{k}\|^2}{\tilde{\varepsilon}}\tilde{\phi} = \eta\tilde{\phi}. \end{aligned} \tag{16}$$

Putting $h_\xi = (1/n)$ and $h_\zeta = (1/m)$, we then obtain from (15) (TM mode) the finite difference scheme

$$\begin{aligned} &- \frac{1}{4\pi^2}\left(\|\boldsymbol{b}_1\|^2 \frac{\tilde{\phi}_{j+1,l} - 2\tilde{\phi}_{j,l} + \tilde{\phi}_{j-1,l}}{h_\xi^2} + \|\boldsymbol{b}_2\|^2 \frac{\tilde{\phi}_{j,l+1} - 2\tilde{\phi}_{j,l} + \tilde{\phi}_{j-1,l}}{h_\zeta^2} \right. \\ &\left. + 2\boldsymbol{b}_1 \cdot \boldsymbol{b}_2 \frac{\tilde{\phi}_{j+1,l+1} + \tilde{\phi}_{j-1,l-1} - \tilde{\phi}_{j+1,l-1} - \tilde{\phi}_{j-1,l+1}}{4h_\xi h_\zeta} \right) \\ &- \frac{i}{\pi}\left((\boldsymbol{b}_1 \cdot \boldsymbol{k}) \frac{\tilde{\phi}_{j+1,l} - \tilde{\phi}_{j-1,l}}{2h_\xi} + (\boldsymbol{b}_2 \cdot \boldsymbol{k}) \frac{\tilde{\phi}_{j,l+1} - \tilde{\phi}_{j,l-1}}{2h_\zeta} \right) + \|\boldsymbol{k}\|^2\tilde{\phi}_{j,l} = \eta\tilde{\varepsilon}_{j,l}\tilde{\phi}_{j,l}, \end{aligned} \tag{17}$$

DOI: 10.1685/journal.caim.374

where $\tilde{\phi}_{j,l} = \tilde{\phi}(j/n, l/m) = \phi(j\boldsymbol{a}_1/n, l\boldsymbol{a}_2/m)$. The linear system obtained has the form (8), where D is a diagonal matrix with positive diagonal entries $\tilde{\varepsilon}_{j,l}$ and C is a two-index circulant matrix with eigenvalues [40–42]

$$\begin{aligned}
&\frac{1}{2\pi^2}\left(\frac{\|\boldsymbol{b}_1\|^2}{h_\xi^2}(1-\cos\theta_j)+\frac{\|\boldsymbol{b}_2\|^2}{h_\zeta^2}(1-\cos\varphi_l)+\frac{\boldsymbol{b}_1\cdot\boldsymbol{b}_2}{h_\xi h_\zeta}\sin\theta_j\sin\varphi_l\right)\\
&+\frac{1}{\pi}\left(\frac{\boldsymbol{b}_1\cdot\boldsymbol{k}}{h_\xi}\sin\theta_j+\frac{\boldsymbol{b}_2\cdot\boldsymbol{k}}{h_\zeta}\sin\varphi_l\right)^2+\|\boldsymbol{k}\|^2\\
&=\left\|\boldsymbol{k}+\frac{\sin\theta_j}{2\pi h_\xi}\boldsymbol{b}_1+\frac{\sin\varphi_l}{2\pi h_\zeta}\boldsymbol{b}_2\right\|^2+\frac{1}{\pi^2}\left(\frac{\|\boldsymbol{b}_1\|^2}{h_\xi^2}\sin^4(\tfrac{1}{2}\theta_j)+\frac{\|\boldsymbol{b}_2\|^2}{h_\zeta^2}\sin(\tfrac{1}{2}\varphi_l)\right)\\
&=\|\boldsymbol{k}+j\boldsymbol{b}_1+l\boldsymbol{b}_2\|^2+O(n^{-2}+m^{-2}),
\end{aligned}\tag{18}$$

where $\theta_j = (2\pi j/n)$ $(j = 0, 1, \ldots, n-1)$ and $\varphi_l = (2\pi l/m)$ $(l = 0, 1, \ldots, m-1)$. Consequently, all eigenvalues of C are nonnegative and zero is an eigenvalue if and only if $k_x = k_y = j = l = 0$. Moreover, they converge to the exact eigenvalues of (5) with periodic conditions if $\varepsilon(x, y) \equiv 1$. For TE modes we get from (16) the finite difference scheme

$$\begin{aligned}
&\tfrac{1}{2}\left[\frac{1}{\tilde{\varepsilon}_{j+1,l}}+\frac{1}{\tilde{\varepsilon}_{j,l}}\right]\left[-\frac{\|\boldsymbol{b}^1\|^2}{4\pi^2h_\xi^2}+\frac{\boldsymbol{b}^1\cdot\boldsymbol{k}}{2\pi i h_\xi}\right]\tilde{\phi}_{j+1,l}-\tfrac{1}{2}\left[\frac{1}{\tilde{\varepsilon}_{j,l}}+\frac{1}{\tilde{\varepsilon}_{j-1,l}}\right]\left[\frac{\|\boldsymbol{b}^1\|^2}{4\pi^2h_\xi^2}+\frac{\boldsymbol{b}^1\cdot\boldsymbol{k}}{2\pi i h_\xi}\right]\tilde{\phi}_{j-1,l}\\
&+\tfrac{1}{2}\left[\frac{1}{\tilde{\varepsilon}_{j,l+1}}+\frac{1}{\tilde{\varepsilon}_{j,l}}\right]\left[-\frac{\|\boldsymbol{b}^2\|^2}{4\pi^2h_\zeta^2}+\frac{\boldsymbol{b}^2\cdot\boldsymbol{k}}{2\pi i h_\zeta}\right]\tilde{\phi}_{j,l+1}-\tfrac{1}{2}\left[\frac{1}{\tilde{\varepsilon}_{j,l}}+\frac{1}{\tilde{\varepsilon}_{j,l-1}}\right]\left[\frac{\|\boldsymbol{b}^2\|^2}{4\pi^2h_\zeta^2}+\frac{\boldsymbol{b}^2\cdot\boldsymbol{k}}{2\pi i h_\zeta}\right]\tilde{\phi}_{j,l-1}\\
&-\frac{\boldsymbol{b}^1\cdot\boldsymbol{b}^2}{32\pi^2h_\xi h_\zeta}\left[\left(\frac{1}{\tilde{\varepsilon}_{j,l+1}}+\frac{2}{\tilde{\varepsilon}_{j,l}}+\frac{1}{\tilde{\varepsilon}_{j+1,l}}\right)\tilde{\phi}_{j+1,l+1}+\left(\frac{1}{\tilde{\varepsilon}_{j-1,l}}+\frac{2}{\tilde{\varepsilon}_{j,l}}+\frac{1}{\tilde{\varepsilon}_{j,l-1}}\right)\tilde{\phi}_{j-1,l-1}\right.\\
&\left.-\left(\frac{1}{\tilde{\varepsilon}_{j,l+1}}+\frac{2}{\tilde{\varepsilon}_{j,l}}+\frac{1}{\tilde{\varepsilon}_{j-1,l}}\right)\tilde{\phi}_{j-1,l+1}-\left(\frac{1}{\tilde{\varepsilon}_{j,l-1}}+\frac{2}{\tilde{\varepsilon}_{j,l}}+\frac{1}{\tilde{\varepsilon}_{j+1,l}}\right)\tilde{\phi}_{j+1,l-1}\right]\\
&+\left\{\tfrac{1}{4}\left[\frac{1}{\tilde{\varepsilon}_{j+1,l}}+\frac{2}{\tilde{\varepsilon}_{j,l}}+\frac{1}{\tilde{\varepsilon}_{j-1,l}}\right]\left[\frac{\|\boldsymbol{b}^1\|^2}{2\pi^2h_\xi^2}+k_x^2\right]\right\}\tilde{\phi}_{j,l}\\
&+\left\{\tfrac{1}{4}\left[\frac{1}{\tilde{\varepsilon}_{j,l+1}}+\frac{2}{\tilde{\varepsilon}_{j,l}}+\frac{1}{\tilde{\varepsilon}_{j-1,l}}\right]\left[\frac{\|\boldsymbol{b}^2\|^2}{2\pi^2h_\zeta^2}+k_y^2\right]\right\}\tilde{\phi}_{j,l}=\eta\tilde{\phi}_{j,l},
\end{aligned}\tag{19}$$

where $\tilde{\phi}_{j,l} = \tilde{\phi}(j/n, l/m) = \phi(j\boldsymbol{a}_1/n, l\boldsymbol{a}_2/m)$.

In each of our numerical experiments the matrices C of systems (17) and (19) have been positive definite for each $\boldsymbol{k} \neq (0, 0)$ and singular for $k_x = k_y = 0$. For this reason we conjecture that this property holds true as in the rectangular case.

3. Analysis of the matrix systems.

The linear systems (9) (TM rectangular), (12) (TE rectangular), (17) (TM oblique), and (19) (TE oblique) obtained by applying the FDFD method all have the form

$$(C - \eta D)\boldsymbol{\phi} = 0, \tag{20}$$

where C is a nonnegative hermitian matrix and D is a positive definite hermitian matrix, both of order mn. The generalized eigenvalues of the pencil $C-\eta D$, i.e., the values of η for which (20) has a nontrivial solution, coincide with the eigenvalues of the nonnegative hermitian matrix $D^{-1/2}CD^{-1/2}$ and are therefore nonnegative.

Let us first state the following monotonicity result on the eigenvalues of linear pencils of the type (20). Its proof can easily be derived from the minimax characterization of the eigenvalues [43, Thm. 8.7.1].

Theorem 3.1 (Courant-Fischer). *Let C_1 and C_2 be nonnegative hermitian matrices and D_1 and D_2 positive definite hermitian matrices having the same order N. Suppose that, for each $\boldsymbol{\phi} \in \mathbb{C}^N$,*

$$(C_1\boldsymbol{\phi}, \boldsymbol{\phi}) \geq (C_2\boldsymbol{\phi}, \boldsymbol{\phi}), \tag{21a}$$

$$(D_1\boldsymbol{\phi}, \boldsymbol{\phi}) \leq (D_2\boldsymbol{\phi}, \boldsymbol{\phi}). \tag{21b}$$

Suppose $\lambda_1^s \leq \lambda_2^s \leq \ldots \leq \lambda_N^s$ denote the eigenvalues of the pencil $C_s - \eta D_s$, where $s = 1, 2$. Then

$$\lambda_r^1 \geq \lambda_r^2, \qquad r = 1, 2, \ldots, N. \tag{22}$$

Proof. By the minimax principle [43, Thm. 8.3.2], we have

$$\lambda_r^s = \max_{\mathcal{L}_r} \min_{0 \neq \boldsymbol{\phi} \in \mathcal{L}_r} \frac{(C_s\boldsymbol{\phi}, \boldsymbol{\phi})}{(D_s\boldsymbol{\phi}, \boldsymbol{\phi})}, \qquad r = 1, 2, \ldots, N, \quad s = 1, 2,$$

where $\mathcal{L}_r$ is a linear subspace of $\mathbb{C}^N$ of dimension $N - r + 1$. Now the conclusion (22) is immediate from (21). □

The linear systems of the type (20) obtained by using the FDFD method are composed of matrices C and D of order mn which depend on the dielectric constant ε. When ε is increasing, for each $\boldsymbol{\phi} \in \mathbb{C}^{mn}$ the scalar product $(C\boldsymbol{\phi}, \boldsymbol{\phi})$ decreases and the scalar product $(D\boldsymbol{\phi}, \boldsymbol{\phi})$ increases. As a result of Theorem 3.1, the r-th smallest eigenvalue of the pencil $C - \eta D$ decreases ($r = 1, \ldots, mn$).

DOI: 10.1685/journal.caim.374

Let us now consider the detailed structure of the matrices C and D obtained by applying the FDFD method. The matrices C and D are two-index in the sense that their elements can be written as $C_{(j,l),(j',l')}$ and $D_{(j,l),(j',l')}$, where (j,l) and (j',l') are as in (10).

In the TM mode the FDFD method leads to a linear system of the type (20), where C is a two-index *circulant* tridiagonal matrix and D is a positive diagonal matrix. Instead, in the TE mode the FDFD method leads to a linear system of the form (20), where C is a two-index *noncirculant* tridiagonal matrix and D is the identity matrix. In all four cases considered, the matrix C is nonnegative hermitian and the matrix D is positive definite hermitian.

In homogeneous media ($\varepsilon(x,y) \equiv \varepsilon$ constant) it is possible to solve the linear systems arising from the FDFD method explicitly. Since the corresponding TM and TE modes lead to the same linear system (20) (except for an irrelevant factor ε in both C and D), we discuss only the TM mode. In the FDFD-TM case the eigenvalues of (20) are those of the two-index circulant matrix divided by ε. Taking the limits of (13) (FDFD-TM, rectangular crystal) and (18) (FDFD-TM, oblique crystal), we obtain, apart from a term of the order of $O(n^{-2}+m^{-2})$, the exact eigenvalues η which can be evaluated by separation of variables.

4. Numerical results.

In this section we present numerical results on the band spectra of 2D photonic crystals obtained by using the FDFD method, illustrated in Sec. 2. These results are compared with each other and with those obtained by using the MIT Photonic-Bands software which can be downloaded from the website *http://ab-initio.mit.edu/photons/index.html*

All computations in this paper were performed using MatLab (version 7.11.0) on an AMD46 computer equipped with an Intel Core i7 860 processor with a speed of 2.80 GHz. We developed a MatLab toolbox, called *2DPhotonics*, which is available upon request.

The photonic crystal configurations considered in this section are those depicted in Fig. 1 in the case of a rectangular lattice and in Fig. 2 in the case of an oblique lattice, both considered before in [1]. More precisely, as in [1], we considered the following configurations of photonic crystals:

a) a square distribution of dielectric rods ($\varepsilon = 8.9$, radius $r = 0.2a$) embedded in air, a being the lattice constant (top half of Fig. 1);
b) a square distribution of dielectric veins ($\varepsilon = 8.9$, thickness $0.165a$) embedded in air, a being the lattice constant (bottom half of Fig. 1);
c) a triangular array of air columns drilled in a dielectric substrate

(radius $r = 0.48a$, $\varepsilon = 13$), a being the lattice constant (Fig. 2).

In the cases a)-c) the band spectra in the TM and the TE modes have been computed by using our FDFD method. For a comparison between our results and the ones most quoted in the literature, we reported in Tables 1-4 the TM and TE spectra computed by our method and the MIT Photonic-Band software mentioned above.

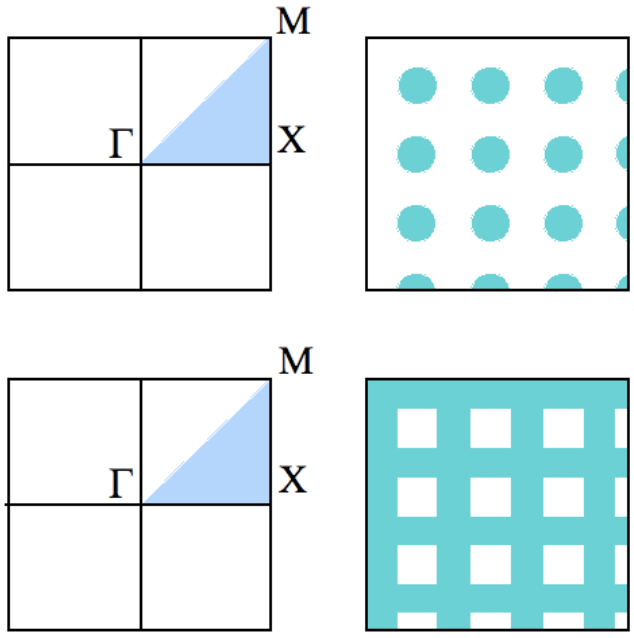

Figure 1. The top half of the figure shows a photonic crystal composed of a square distribution of dielectric rods ($\varepsilon = 8.9$, $r = 0.2a$) embedded in air and the corresponding Brillouin zone. The Γ-point corresponds to $k_x = k_y = 0$, the X-point to $k_x = \pi/a$ and $k_y = 0$ and finally at the M-point one has $k_x = k_y = \pi/a$, a being either period. The bottom half of the figure shows a photonic crystal composed of a square distribution of dielectric veins ($\varepsilon = 8.9$, thickness $0.165a$) in air and the corresponding Brillouin zone.

4.1. *Two rectangular lattices.*

Firstly we note that, as $\varepsilon(x, y)$ is invariant under the group of automorphisms of the square lattice, it is sufficient to choose the wavevector $\boldsymbol{k}$ in one eighth of the Brillouin zone [4] (Fig. 1). As a consequence we computed the band spectrum by solving the eigenvalue problems (9), (12) for different wavevectors varying, as specified below, on the boundary of the blue region shown in Fig. 1:

1. $k_x \in [0, \pi/a], \quad k_y = 0,$

DOI: 10.1685/journal.caim.374

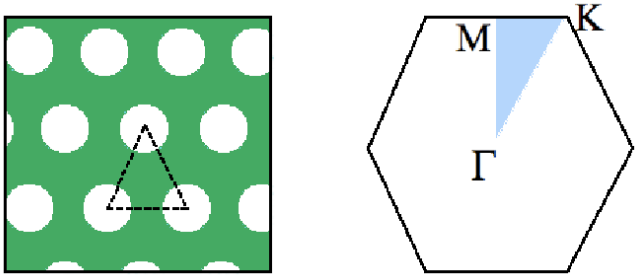

Figure 2. The figure shows a photonic crystal made of a triangular array of air columns drilled in a dielectric substrate ($r = 0.48a$, $\varepsilon = 13$) and the corresponding Brillouin zone. The Γ-point corresponds to $k_x = k_y = 0$, the M-point to $k_x = 0$ and $k_y = 2\pi/(\sqrt{(}3)a)$ and finally at the K-point one has $k_x = 2\pi/(3a)$ and $k_y = 2\pi/(\sqrt{(}3)a)$, where the period parallelogram is a rhombus with sides a.

2. $k_x = \pi/a, \quad k_y \in [0, \pi/a]$,
3. $k_x \in [0, \pi/a], \quad k_y \in [0, \pi/a]$.

$\boldsymbol{k}$		TM		TE	
k_x	k_y	FE	FDFD	FE	FDFD
0.0	0.0	0.000000	0.000000	0.000000	0.000000
0.2	0.0	0.139465	0.139226	0.180051	0.180634
0.4	0.0	0.254053	0.254376	0.353842	0.353964
0.5	0.1	0.280546	0.280765	0.428562	0.428803
0.5	0.3	0.306291	0.306913	0.506456	0.506872
0.5	0.5	0.324533	0.324677	0.553457	0.553002
0.3	0.3	0.268305	0.268478	0.378416	0.378652
0.1	0.1	0.099665	0.099742	0.127688	0.127521

Since in our FDFD method a regular grid is used and recalling the monotonicity property proved in Sec. 3, the dielectric constant $\varepsilon(x, y)$ has been sampled both in a defect and in an excess approximation and their arithmetic average is assumed to be the effective approximation. For the sake of clarity, let us explain this procedure for the case where the photonic crystal is composed of dielectric rods (top half of Fig. 2). The dielectric constant has been sampled first in a defect approximation where the dielectric values different from one have been selected for the grid points inside the disk with radius $r = 0.2a$, and then in an excess approximation where the dielectric values equal to one have been selected for the grid points outside the disk with radius $r = 0.2a$. The right-hand side of Fig. 3 shows the dielectric constant distribution on a 20×20 regular grid both in the defect and

$\boldsymbol{k}$		TM		TE	
k_x	k_y	FE	FDFD	FE	FDFD
0.0	0.0	0.633721	0.633134	0.827543	0.827157
0.2	0.0	0.636577	0.636717	0.758997	0.758070
0.4	0.0	0.641358	0.641721	0.710275	0.710756
0.5	0.1	0.631219	0.631115	0.698984	0.698468
0.5	0.3	0.580532	0.580332	0.651086	0.651573
0.5	0.5	0.552753	0.552103	0.601662	0.601329
0.3	0.3	0.579892	0.579910	0.655872	0.656392
0.1	0.1	0.625651	0.625721	0.784024	0.784706

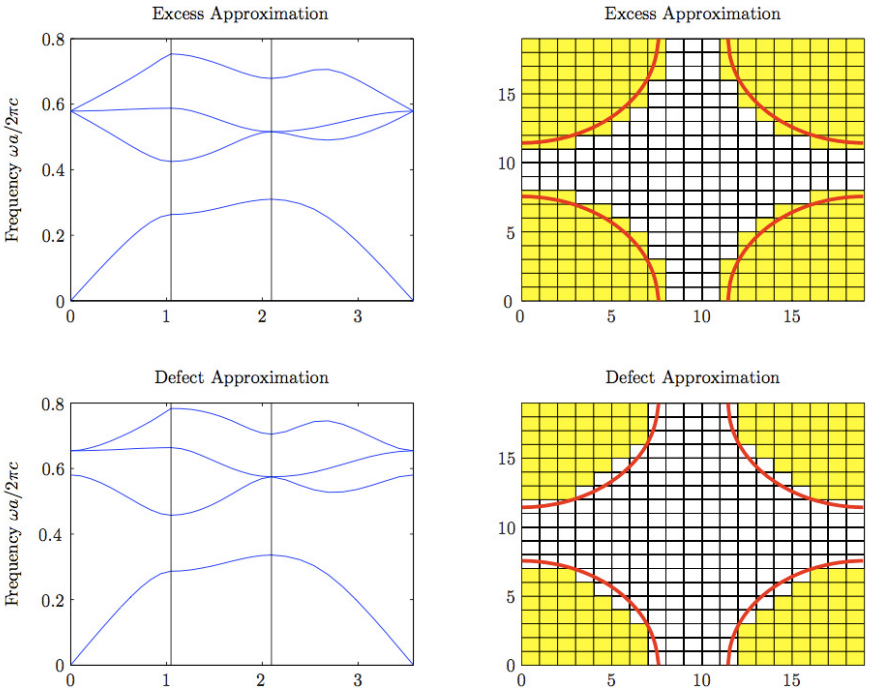

Figure 3. The left half of the figure shows the band structure corresponding to the defect and excess grid approximation for TM modes for the photonic crystal made of dielectric rods embedded in air (top half of Fig. 2). The corresponding 20×20 grids are shown on the right half.

the excess approximations and the left-hand side shows the corresponding band spectra.

As proved in Sec. 3, the absolute and relative errors behave like $n^{-2} + m^{-2}$ (where n and m are the numbers of grid points in the x and y direction, respectively) when $\varepsilon(x, y)$ is constant (homogeneous case). Our

DOI: 10.1685/journal.caim.374

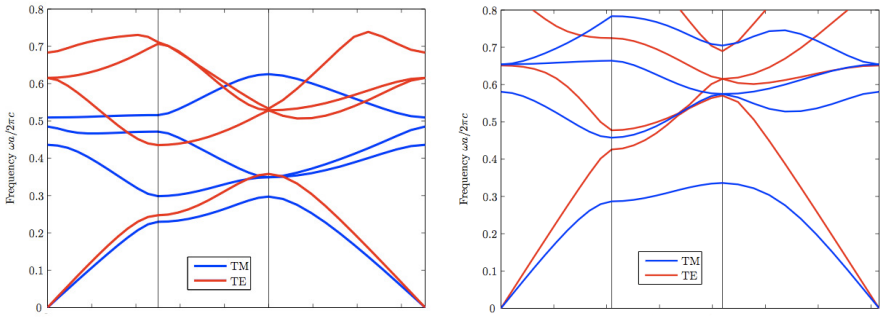

Figure 4. The figure on the right shows the TM and TE spectra for a square array of dielectric columns in air (top half of Fig. 1), while the figure on the left shows the TM and TE spectra for a square array of dielectric veins in air (bottom half of Fig. 1).

$\boldsymbol{k}$		TM		TE	
k_x	k_y	FE	FDFD	FE	FDFD
0.0	0.0	0.000000	0.000000	0.000000	0.000000
0.2	0.0	0.106607	0.106311	0.123318	0.123706
0.4	0.0	0.203708	0.203262	0.226933	0.226088
0.5	0.1	0.233776	0.233182	0.255797	0.255031
0.5	0.3	0.264042	0.264648	0.311166	0.311463
0.5	0.5	0.297267	0.297914	0.357971	0.357276
0.3	0.3	0.216367	0.216914	0.257825	0.257496
0.1	0.1	0.141421	0.141637	0.088332	0.088046

$\boldsymbol{k}$		TM		TE	
k_x	k_y	FE	FDFD	FE	FDFD
0.0	0.0	0.485054	0.485498	0.615396	0.615744
0.2	0.0	0.466427	0.466223	0.631361	0.631639
0.4	0.0	0.470366	0.470268	0.676816	0.676011
0.5	0.1	0.453313	0.453083	0.681243	0.681899
0.5	0.3	0.392038	0.392523	0.588334	0.588583
0.5	0.5	0.349106	0.349896	0.528361	0.528095
0.3	0.3	0.389044	0.389547	0.551563	0.551149
0.1	0.1	0.421794	0.421188	0.602741	0.602809

numerical experiments confirm this result. In particular, taking a 60×60 grid we obtained a 10^{-3} error. As the exact eigenvalues are not known in the inhomogeneous case, we compared the results obtained by our method with those obtained by Joannopoulos et al. [1] using the MIT Photonic-Bands

software (FE method). The numerical results thus obtained are reported in Tables 1-4, where the eigenvalues shown have been computed using a 100×100 grid for the FDFD method and a 128×128 grid for the FE method. In each table, the eigenvalues thus obtained and associated to the wavevectors $\boldsymbol{k}$ reported, are labeled as FE and FDFD, respectively. The results illustrate that the two methods give essentially the same numerical results.

4.2. *An oblique lattice.*

We computed the spectrum solving the eigenvalue problems (17) and (19) for fixed $\boldsymbol{k}$ values. This time we are dealing with an oblique lattice and in this case it is sufficient [1] to consider $\boldsymbol{k}$ varying on the boundary of the blue region of the Brillouin zone (Fig. 2) as follows:

1. $k_x = 0, \quad k_y \in [0, 2\pi/(\sqrt{3}a)]$,
2. $k_x \in [0, 2\pi/(3a)], \quad k_y = 2\pi/(\sqrt{3}a)$,
3. $k_x \in [2\pi/(3a), 0], \quad k_y \in [2\pi/(\sqrt{3}a), 0]$.

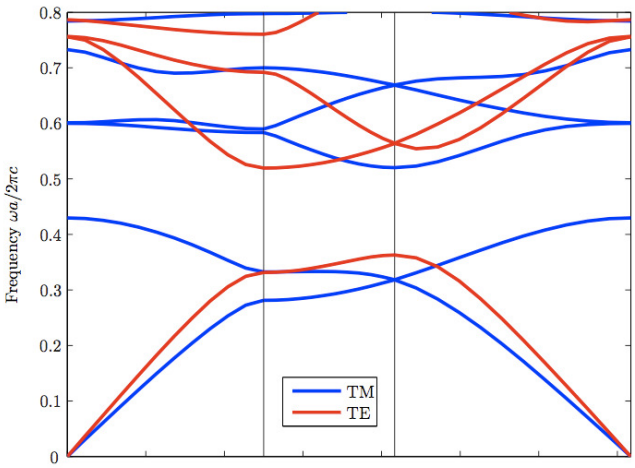

Figure 5. TM and TE spectra obtained by the FDFD method for photonic crystal made of a triangular distribution of rods embedded in a dielectric medium (see Fig. 2).

As in Subsec. 4.1, the dielectric function $\varepsilon(x, y)$ has been sampled first in a defect approximation and then in an excess approximation, but this time for $r = 0.48a$. We considered a 60×60 grid. The corresponding band structures for both the TM and TE modes are shown in Fig. 5. In this figure the results obtained by using the FE software mentioned above have

DOI: 10.1685/journal.caim.374

not been plotted, as they are visually indistinguishable from the results obtained by our FDFD method.

5. Conclusions.

In this paper we propose a finite difference frequency domain method to determine the spectra of two-dimensional photonic crystals. We also compare the results thus obtained with each other and with those obtained by the MPB software [1]. Our numerical experiments illustrate that the two methods produce essentially the same results in all cases considered. This does not imply that the methods used are equally effective. Actually, the results could be quite different, especially when either the dielectric function $\varepsilon(x, y)$ is strongly variable on the elementary cell or a larger number of spectral bands has to be computed.

We note that the FDFD method, when applied to homogeneous media, gives the exact results for the TM and TE modes, which is not true when we apply the FE method. Moreover, whereas the FE method, when applied to discontinuous media, requires a regularization of the dielectric function $\varepsilon(x, y)$ in order to speed up the convergence of the Fourier series, our method does not require any regularization of $\varepsilon(x, y)$, which simplifies the use of the method and makes it easily extendable to the 3D case, because the 3D domains involved are parallelepipeds and hence quite regular. Moreover, the FDFD method generates eigenvalues (see Sec. 3) that are decreasing with respect to the dielectric function, something which is not clear in the case of the FE method. It is worthwhile to note that, from the numerical point of view, this monotonicity property can be used to obtain error estimates for the numerical results.

Acknowledgments.

The research was partially supported by the Italian Ministery of Education and Research (MIUR) under PRIN grant No. 2006017542–003, by INdAM, and by the Autonomous Region of Sardinia under grant L.R.7/2007 "Promozione della Ricerca Scientifica e della Innovazione Tecnologica in Sardegna."

REFERENCES

1. J. Joannopoulos, R. Meade, and J. Winn, *Photonic Crystals, Molding the flow of light.* Princeton: Princeton University Press, 2006.
2. K. Sakoda, *Optical Properties of Photonic Crystals.* Berlin and New York: Springer, 2001.

3. M. Born and E. Wolf, *Principles of Optics. Electromagnetic Theory of Propagation, Interference and Diffrection of Light.* London: Cambridge University Press, 1999.
4. L. Brillouin, *Wave Propogation in Periodic Structures.* New York: Dover Publ., 1953.
5. Z. Zhang and S. Satpathy, Electromagnetic wave propagation in periodic structures: Bloch wave solution of maxwell's equations, *Phys. Rev. Lett.*, vol. 65, pp. 2650–2653, 1990.
6. K. Ho, C. Chan, and C. Soukoulis, Existence of a photonic gap in periodic dielectric structures, *Phys. Rev. Lett.*, vol. 65, pp. 3152–3155, 1990.
7. M. Philal and A. Maradudin, Photonic band structure of two-dimensional systems: The triangular lattice, *Phys. Rev. B*, vol. 44, pp. 8565–8571, 1991.
8. H. Sözüer and J. Haus, Photonic bands: Convergence problems with the planewave method, *Phys. Rev. B*, vol. 45, pp. 13962–13972, 1992.
9. P. Villeneuve and M. Piché, Photonic band gaps in two-dimensional square and hexagonal lattices, *Phys. Rev. B*, vol. 46, pp. 4969–4972, 1992.
10. K. Leung and Y. Qiu, Multiple-scattering calculation of the two-dimensional photonic band structure, *Phys. Rev. B*, vol. 48, pp. 7767–7771, 1993.
11. C. Chan, Q. Yu, and K. Ho, Order-n spectral method for electromagnetic waves, *Phys. Rev. B*, vol. 51, pp. 16635–16642, 1995.
12. A. Ward and J. Pendry, Refraction and geometry in maxwell's equations, *J. Mod. Opt.*, vol. 43, pp. 773–793, 1996.
13. A. Ward and J. Pendry, Calculating photonic green's functions using a nonorthogonal finite-difference time-domain method, *Phys. Rev. B*, vol. 58, pp. 7252–7259, 1998.
14. J. Arriaga, A. Ward, and J. Pendry, Order-n photonic band structures for metals and other dispersive materials, *Phys. Rev. B*, vol. 59, pp. 1874–1877, 1999.
15. M. Qiu and S. He, A nonorthogonal finite-difference time-domain method for computing the band structure of a two-dimensional photonic crystal with dielectric and metallic inclusions, *J. Appl. Phys.*, vol. 87, pp. 8268–8275, 2000.
16. S. He, S. Xiao, L. Shen, J. He, and J. Fu, A new finite-difference time-domain method for photonic crystals consisting of nearly-free-electron metals, *J. Phys A*, vol. 34, pp. 9713–9721, 2001.
17. B. Cowan, Fdtd modeling of photonic crystal fibers, Tech. Rep. ARDB–339, Stanford University, Palo Alto, CA, 2003.

DOI: 10.1685/journal.caim.374

18. J. Pendry and A. MacKinnon, Calculation of photon dispersion relations, *Phys. Rev. Lett.*, vol. 69, pp. 2772–2775, 1992.

19. H. Y. D. Yang, Finite difference analysis of 2-d photonic crystals, *IEEE Trans. on Microwave Theory and Techniques*, vol. 44, pp. 2688–2695, 1996.

20. D. Hermann, M. Frank, K. Busch, , and P. Wölfle, Photonic band structure computations, *Opt. Express*, vol. 8, pp. 167–172, 2000.

21. J.-K. Hwang, S.-B. Hyun, H.-Y. Ryu, and Y.-H. Lee, Resonant modes of two-dimensional photonic bandgap cavities determined by the finite-element method and by use of the anisotropic perfectly matched layer boundary condition, *J. Opt. Soc. Am. B*, vol. 15, pp. 2316–2324, 1998.

22. D. Dobson, An efficient method for band structure calculations in 2d photonic crystals, *J. Comp. Phys.*, vol. 149, pp. 363–376, 1999.

23. W. Axmann and P. Kuchment, An efficient finite element method for computing spectra of photonic and acoustic band-gap materials, *J. Comp. Phys.*, vol. 150, pp. 468–481, 1999.

24. G. Pelosi, A hybrid fem-based procedure for the scattering from photonic crystals illuminated by a gaussian beam, *IEEE Trans. on Antennas and Propagation*, vol. 48, pp. 973–980, 2000.

25. D. Dobson, J. Gopalakrishnan, and J. Pasciak, An efficient method for band structure calculations in 3d photonic crystals, *J. Comp. Phys.*, vol. 161, pp. 668–679, 2000.

26. B. Hiett, J. Generowicz, S. Cox, M. Molinari, D. Beckett, and K. Thomas, Application of finite element methods to photonic crystal modelling, *IEEE Proc.-Sci. Meas. Technol.*, vol. 149, pp. 293–296, 2002.

27. W. J. Kim and J. O'Brien, Optimization of a two-dimensional photonic-crystal waveguide branch by simulated annealing and the finite element method, *J. Opt. Soc. Am. B*, vol. 21, pp. 289–295, 2004.

28. D. Boffi, M. Conforti, and L. Gastaldi, Modified edge finite elements for photonic crystals, *Numer. Math.*, vol. 105, pp. 249–266, 2006.

29. V. Hoang, M. Plum, and C. Wieners, A computer assisted proof for photonic band gaps, *Z. angew. Math. Phys.*, vol. 60, pp. 1035–1052, 2009.

30. E. Moreno, D. Erni, and C. Hafner, Band structure computations of metallic photonic crystals with the multiple multipole method, *Phys. Rev. B*, vol. 65, pp. 155120, 10 pp., 2002.

31. O. Martin and C. Girard, Generalized field propagator for arbitrary finite-size photonic band gap structures, *Phys. Rev. Lett.*, vol. 82, pp. 315–318, 1999.

32. X. Wang, X.-G. Zhang, Q. Yu, and B. Harmon, Multiple-scattering theory for electromagnetic waves, *Phys. Rev. B*, vol. 47, pp. 4161–4167,

1993.

33. W. Zhang, C. Chan, and P. Sheng, Multiple scattering theory and its application to photonic band gap systems consisting of coated spheres, *Opt. Express*, vol. 8, pp. 203–208, 2000.
34. K. Sakoda, Optical transmittance of a two-dimensional triangular photonic lattice, *Phys. Rev. B*, vol. 51, pp. 4672–4675, 1995.
35. K. Sakoda, Transmittance and bragg reflectivity of two-dimensional photonic lattices, *Phys. Rev. B*, vol. 52, pp. 8992–9002, 1995.
36. P. Contu, *Band Structure in Photonic Crystals. Analytical and Numerical Methods*. PhD thesis, Department of Mathematics and Computer Science, University of Cagliari, 2011.
37. A. Mitchell and D. Griffiths, *The Finite Difference Method in Partial Differential Equations*. New York: Wiley-Blackwell, 1980.
38. J. Thomas, *Numerical Partial Differential Equations: Finite Difference Methods*. No. 22 in Springer Texts in Applied Mathematics, Berlin and New York: Springer, 1995.
39. G. Smith, *Numerical Solution of Partial Differential Equations: Finite Difference Methods*. Oxford: Oxford Univ. Press, 1985.
40. P. I. Davis, *Circulant Matrices*. New York: Wiley-Interscience, 1979.
41. C. van der Mee, G. Rodriguez, and S. Seatzu, Fast computation of two-level circulant preconditioners, *Numerical Algorithms*, vol. 41, no. 3, pp. 275–295, 2006.
42. C. van der Mee, G. Rodriguez, and S. Seatzu, Fast superoptimal preconditioning of multiindex toeplitz matrices, *Linear Algebra and its Applications*, vol. 418, pp. 576–590, 2006.
43. P. Lancaster and M. Tismenetsky, *The Theory of Matrices*. Orlando etc.: Academic Press, 1985.